



Universiteit
Leiden
The Netherlands

Optimizing mutation and fusion detection in NSCLC by sequential DNA and RNA sequencing

Cohen, D.; Hondelink, L.M.; Solleveld-Westerink, N.; Uljee, S.M.; Ruano, D.; Cleton-Jansen, A.M.; ... ; Wezel, T. van

Citation

Cohen, D., Hondelink, L. M., Solleveld-Westerink, N., Uljee, S. M., Ruano, D., Cleton-Jansen, A. M., ... Wezel, T. van. (2020). Optimizing mutation and fusion detection in NSCLC by sequential DNA and RNA sequencing. *Journal Of Thoracic Oncology*, 15(6), 1000-1014.
doi:10.1016/j.jtho.2020.01.019

Version: Publisher's Version
License: [Creative Commons CC BY-NC-ND 4.0 license](https://creativecommons.org/licenses/by-nc-nd/4.0/)
Downloaded from: <https://hdl.handle.net/1887/3184036>

Note: To cite this publication please use the final published version (if applicable).

Optimizing Mutation and Fusion Detection in NSCLC by Sequential DNA and RNA Sequencing



Danielle Cohen, MD, PhD,^{a,*} Liesbeth M. Hondelink, MD,^a
Nienke Solleveld-Westerink, PhD,^a Sandra M. Uljee, BSc,^a Dina Ruano, PhD,^a
Anne-Marie Cleton-Jansen, PhD,^a Jan H. von der Thüsen, MD, PhD,^a
S. Rajen S. Ramai, MD,^b Pieter E. Postmus, MD, PhD,^b
Jacob F. Graadt van Roggen, MD, PhD,^c Bart P. C. Hoppe, MD,^d
Pieter C. Clahsen, MD, PhD,^e Klaartje W. Maas, MD, PhD,^f
Els J. M. Ahsmann, MD, PhD,^g Alexandra ten Heuvel, MD,^h Frank Smedts, MD, PhD,ⁱ
Ronald N. van Rossem, MD,^j Tom van Wezel, PhD^a

^aDepartment of Pathology, Leiden University Medical Centre (LUMC), Leiden, The Netherlands

^bDepartment of Pulmonology, Leiden University Medical Centre (LUMC), Leiden, The Netherlands

^cDepartment of Pathology, Alrijne Hospital, Leiderdorp, The Netherlands

^dDepartment of Pulmonology, Alrijne Hospital, Leiderdorp, The Netherlands

^eDepartment of Pathology, Haaglanden Medical Centre (HMC), Den Haag, The Netherlands

^fDepartment of Pulmonology, Haaglanden Medical Centre (HMC), Den Haag, The Netherlands

^gDepartment of Pathology, Groene Hart Hospital (GHZ), Gouda, The Netherlands

^hDepartment of Pulmonology, Groene Hart Hospital (GHZ), Gouda, The Netherlands

ⁱDepartment of Pathology, Reinier de Graaf gasthuis (RdGG), Delft, The Netherlands

^jDepartment of Pulmonology, Reinier de Graaf gasthuis (RdGG), Delft, The Netherlands

Received 28 August 2019; revised 23 January 2020; accepted 24 January 2020

Available online - 31 January 2020

ABSTRACT

Introduction: Frequently, patients with locally advanced or metastatic NSCLC are screened for mutations and fusions. In most laboratories, molecular workup includes a multitude of tests: immunohistochemistry (*ALK*, *ROS1*, and programmed death-ligand 1 testing), DNA sequencing, in situ hybridization for fusion, and amplification detection. With the fast-emerging new drugs targeting specific fusions and exon-skipping events, this procedure harbors a growing risk of tissue exhaustion.

Methods: In this study, we evaluated the benefit of anchored, multiplexed, polymerase chain reaction-based targeted RNA sequencing (RNA next-generation sequencing [NGS]) in the identification of gene fusions and exon-skipping events in patients, in which no pathogenic driver mutation was found by DNA-based targeted cancer hotspot NGS (DNA NGS). We analyzed a cohort of stage IV NSCLC cases from both in-house and referral hospitals, consisting 38.5% cytology samples and 61.5% microdissected histology samples, mostly core needle biopsies. We compared molecular findings in a parallel workup (DNA NGS and RNA NGS, cohort 1, n = 198) with a sequential workup (DNA NGS followed by RNA NGS in

selected cases, cohort 2, n = 192). We hypothesized the sequential workup to be the more efficient procedure.

Results: In both cohorts, a maximum of one oncogenic driver mutation was found per case. This is in concordance with large, whole-genome databases and suggests that it is safe to omit RNA NGS when a clear oncogenic driver is identified in DNA NGS. In addition, this reduced the number of necessary RNA NGS to only 53% of all cases. The tumors

*Corresponding author.

Drs. Cohen and Hondelink equally contributed to this work.

Disclosure: Dr. Postmus reports grants and personal fees from Boehringer Ingelheim, Merck Sharp & Dohme Corp., Eli Lilly, Bristol-Myers Squibb, Precision Oncology, Philips, Seattle Genetics, and AstraZeneca, outside the submitted work. The remaining authors declare no conflict of interest.

Address for correspondence: Danielle Cohen, MD, PhD, Department of Pathology, Leiden University Medical Centre, Postbus 9600, Room P2-3, Albinusdreef 2, 2300 RC Leiden, The Netherlands. E-mail: d.cohen@lumc.nl

© 2020 International Association for the Study of Lung Cancer. Published by Elsevier Inc. This is an open access article under the CC BY-NC-ND license (<http://creativecommons.org/licenses/by-nc-nd/4.0/>).

ISSN: 1556-0864

<https://doi.org/10.1016/j.jtho.2020.01.019>

of never smokers, however, were enriched for fusions and exon-skipping events (32% versus 4% in former and current smokers, $p = 0.00$), and therefore benefited more often from the shorter median turnaround time of the parallel approach (15 d versus only 9 d in the parallel workup).

Conclusions: We conclude that sequentially combining DNA NGS and RNA NGS is the most efficient strategy for mutation and fusion detection in smoking-associated NSCLC, whereas for never smokers we recommend a parallel approach. This approach was shown to be feasible on small tissue samples including for cytology tests, can drastically reduce the complexity and cost of molecular workup, and also provides flexibility in the constantly evolving landscape of actionable targets in NSCLC.

© 2020 International Association for the Study of Lung Cancer. Published by Elsevier Inc. This is an open access article under the CC BY-NC-ND license (<http://creativecommons.org/licenses/by-nc-nd/4.0/>).

Keywords: NSCLC; Molecular diagnostics; RNA sequencing; DNA sequencing; Next-generation sequencing

Introduction

The incidence of lung cancer worldwide is high, with more than two million new cases diagnosed in 2018.¹ Most patients present with advanced-stage, unresectable disease. The 5-year survival rate in metastatic disease is only 4.7%, making lung cancer the number one cause of cancer deaths globally.^{1,2}

In current practice, all patients with locally advanced or metastatic NSCLC (nonsquamous type) should be tested for pathogenic driver mutations in *EGFR*,^{3,4} *BRAF*,⁵⁻⁷ *ERBB2*,^{8,9} *KRAS*,^{10,11} and *MET* (including exon 14 skipping)¹²⁻¹⁵; amplifications in *EGFR*,^{16,17} *ERBB2*, and *MET*¹²; fusions in *RET*,¹⁸⁻²⁰ *ALK*,²¹⁻²³ *NTRK*,^{24,25} and *ROS1*^{26,27}; and for programmed death-ligand 1 (PD-L1) expression.²⁸⁻³¹ This is especially important in NSCLC in nonsmokers, who, as a group, are a distinct molecular entity harboring different driver mutations.³² In the past few years, targeted therapy aimed at specific driver mutations has become possible with increasing frequency, making personalized medicine universally accepted and greatly improving prognosis in advanced metastatic disease.³³⁻³⁹

To facilitate the accompanying need for more extensive molecular diagnostics, there have been major and rapid advances in the field of DNA sequencing. In recent years, next-generation sequencing (NGS) has become a typically used method of molecular diagnostics in daily clinical practice of pathology. Although it is now possible to analyze tumor DNA and RNA on the basis of cytology, histology, and even plasma samples, the limited amount

of tissue for NSCLC diagnostics remains a common problem for molecular pathologists and requires a molecular workup that covers all potential targets, including mutations, fusions, and exon-skipping events, while using as little tissue as possible.

Although many laboratories have switched to DNA NGS for mutation detection, oncogenic fusion detection is most often performed by fluorescence in situ hybridization (FISH) or reverse transcription polymerase chain reaction (PCR), and is limited to one fusion site per amplicon or probe. This method often fails to provide useful information regarding the fusion partner and the breakpoint; in FISH, it is not possible to identify the fusion partner, and in reverse transcription PCR, only known partners can be found.^{40,41} The identification of fusion partners is becoming increasingly important because the partners can influence treatment choices and can be of prognostic importance.⁴²⁻⁴⁵

Archer Anchored Multiplex PCR (Archer) technology (RNA NGS) was previously found to efficiently find genomic aberrations, including novel partners, in routine diagnostics for sarcoma⁴⁰ and experimentally in cholangiocarcinoma, glioblastoma, and thyroid carcinoma.⁴¹ In addition, it was noted that RNA NGS was able to identify both known and novel fusion partners for *ALK*,⁴⁶ *ROS1*,^{41,47} *RET*,^{21,41} and *NTRK*,^{26,41} and to identify *MET* exon 14 skipping⁴⁸ in small groups of NSCLC samples.

In a recent study by Benayed et al.,⁴⁹ it was shown that additional Archer-based RNA NGS is required to detect targetable kinase fusions and exon-skipping events that are otherwise missed in their large hybrid capture DNA NGS panel (MSK-IMPACT). This study illustrates that even in large hybrid capture panels, not all fusions and exon-skipping events can be identified owing to the length of introns and blind spots within the targeted areas. Combining hybrid capture DNA NGS with RNA NGS seems the ideal method; however, this procedure is both expensive and probably not feasible in a real-world case-mix of ca. 30% to 40% small histology or cytology samples. Indeed, in this study by Benayed et al.,⁴⁹ only 47% of cases had available tissue left for RNA extraction, suggesting the need for improvement.

In addition, implementing NGS panels in daily practice can be quite expensive. In large-scale, cost-effectiveness analyses, it has been reported that the mean total cost of targeted DNA-based NGS is estimated to be around €607 per patient.⁵⁰ For RNA-based NGS, large-scale cost-effectiveness analysis has not been performed yet, and we estimated our own costs at €500 to €700 per patient.

We herewith present the route to our current molecular workup of advanced-stage and metastatic NSCLC, combining DNA-based targeted PCR-based NGS (DNA NGS) with Archer-based RNA NGS for the detection

of mutations and genetic translocations in routine diagnostics for advanced NSCLC. Our case-mix includes both in-house cases and cases from referral centers with both cytology samples and microdissected histology cases, mostly small core needle biopsies or transbronchial biopsies.

Materials and Methods

Patients and Samples

For this study, we included all NSCLC samples from March 2018 until January 2019 (n = 390) for which a molecular NSCLC workup was performed before first-line treatment at the Leiden University Medical Center. Cases originated from both in-house and referred patients. Cases referred with a different diagnostic goal (e.g., clonality with a second tumor or osimertinib resistance) were excluded. Both histology and cytology specimens were included. Squamous cell carcinoma and large cell neuroendocrine carcinoma were not included. In some cases, the workup could not be completed owing to tissue exhaustion. These cases were not excluded from this study but analyzed separately.

The parallel workup was executed from March 2018 to September 2018 (n = 192). For these cases, we performed both DNA NGS and RNA NGS in addition to immunohistochemical staining for *ALK*, *ROS1*, and PD-L1. After this 6-month period, we switched from this parallel approach to a sequential approach, performing RNA NGS only when no pathogenic driver mutation in *KRAS*, *BRAF*, *EGFR*, or *ERBB2* (including *ERBB2* amplification) or *MET* exon 14 skipping were found in DNA NGS. The sequential approach was performed from September 2018 until January 2019 (n = 198). These cohorts will be henceforth referred to as cohort 1 (parallel approach) and cohort 2 (sequential approach) (Fig. 1).

All samples were isolated from material that had been formalin-fixed, paraffin embedded (FFPE) and preserved. For hematoxylin and eosin and immunohistochemistry (IHC) staining, 1- to 10- μ m thick slides were cut using a Leica RM2255 Automated Microtome. Staining for *ALK* fusion (clone D5F3, laboratory-developed test), *ROS1* (clone D4D6, laboratory-developed test), and PD-L1 (clone 22C3, laboratory-developed test) was performed using a Dako Omnis immunostainer and Dako EnVision Flex+.

The smoking status was extracted from patient records. Patients who had never smoked or had ceased smoking more than 1 month earlier and had accumulated fewer than 5 pack-years were included in the never-smoker category. If they had smoked in the month before diagnosis, they were included in the current-smoker category. The patients with more than 5 pack-years who had not smoked in the month before diagnosis were included in the former-smoker category.

The turnaround time was measured in molecular diagnostics time in workdays (MD time), MD-to-sign time, and received-to-sign time. MD time is the time from the start of molecular analysis until all the results from all molecular analyses are returned to the pathologist. The MD-to-sign time is the time from the start of molecular analysis until the final report (stating all molecular testing results) is completed and becomes available for the clinician. The received-to-sign time is the time from the receipt of the tissue by the pathology department until the final report is completed.

RNA and DNA Isolation

To isolate RNA and DNA for NGS, we collected tumor cells from FFPE blocks by microdissection in cases of core needle biopsies and cytology cell blocks, or by punching resection material. Five 10- μ m slides were used for the isolation of total nucleic acids from a single extraction process using a tissue preparation system robot (Siemens), as described previously in the literature.⁵¹ The same total nucleic acid sample was used for both the DNA and RNA NGS assays, and in most cases, was sufficient to execute the parallel and sequential workflows without additional isolation. When no tissue block was available or when the tissue block did not contain enough tumor cells, tumor cells were scraped off cytology or hematoxylin and eosin slides. After total nucleic acid isolation, the nucleic acid solution was stored in a freezer at -20°C for use in DNA NGS and subsequent RNA NGS. Material that was no longer needed for molecular diagnostic testing was stored at -70°C for future use.

DNA Next-Generation Sequencing

DNA NGS was performed with a customized Cancer Hotspot Panel, covering hotspots in 75 genes, including *ABL1*, *AKT1*, *ALK*, *APC*, *ARAF*, *ATM*, *BRAF*, *CARD11*, *CD79A*, *CD79B*, *CDH1*, *CDK4*, *CDKN2A*, *CIC*, *CSF1R*, *CTNNB1*, *EGFR*, *EIF1AX*, *ERBB2*, *ERBB3*, *ERBB4*, *EZH2*, *FAK (PTK2)*, *FBXW7*, *FGFR1*, *FGFR2*, *FGFR3*, *FLT3*, *FOXL2*, *GNA11*, *GNAQ*, *GNAS*, *H3F3A*, *H3F3B*, *HNF1A*, *HRAS*, *IDH1*, *IDH2*, *JAK2*, *JAK3*, *KDR*, *KIT*, *KRAS*, *MAP2K1*, *MAP2K2*, *MAP2K4*, *MAP3K1*, *MDM2*, *MED12*, *MET*, *MLH1*, *MPL*, *MUTYH*, *MYC*, *MYD88*, *NOTCH1*, *NPM1*, *NRAS*, *PDGFRA*, *PDGFRB*, *PIK3CA*, *POLE*, *PTEN*, *PTPN11*, *RB1*, *RET*, *SMAD4*, *SMARCB1*, *SMO*, *SRC*, *STK11*, *TP53*, and *VHL*. DNA NGS required 15 ng of input DNA per reaction.

The unaligned bam files generated by the Ion Torrent sequencer were mapped against the human reference genome (GRCh37/hg19) using the TMAP 5.0.7 software with default parameters (<https://github.com/iontorrent/TS>). Subsequently, variant calling was done using the Ion Torrent specific caller, Torrent Variant Caller (TVC)-5.0.2, using the recommended Variant Caller Parameter for Cancer Hotspot Panel version 2.

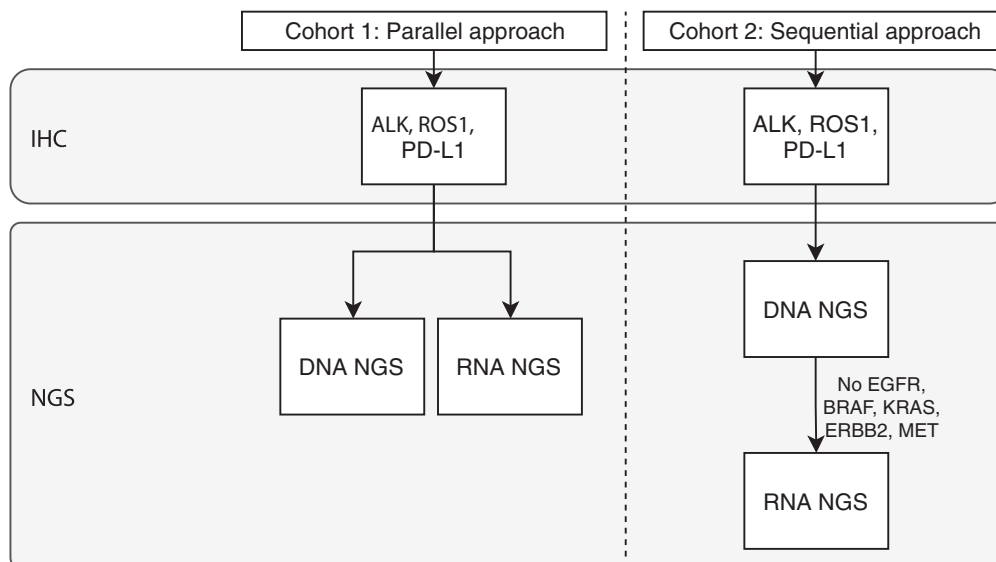


Figure 1. Study design and NSCLC diagnostic workup. Cohort 1 (left): DNA next-generation sequencing (NGS) and RNA NGS in parallel. Cohort 2 (right): DNA NGS and RNA NGS only when no pathogenic mutations are found in *KRAS*, *EGFR*, *BRAF*, and *ERBB2* and no *MET* exon 14 skipping is found (including *ERBB2* and *EGFR* amplification). In both cohorts, immunohistochemical staining for *ROS1*, *ALK*, and programmed death-ligand 1 (PD-L1) was performed before molecular analyses. Both cytology and histology samples were eligible. Nucleic acid was isolated from blocks by microdissection or punching or from slides.

Variant interpretation was done using Genetic Assistant, which assigns functional prediction, conservation scores, and disease-associated information to each variant (http://softgenetics.com/GeneticistAssistant_2.php). Once a pathogenicity classification is assigned to a variant, the same pathogenicity is automatically attributed the next time the variant is observed. Integrative Genomics Viewer was used for visually inspecting variants.⁵²

Chromosomal gains and losses (copy number changes) were also assessed. In short, the median base coverage per amplicon was calculated. The amplicon coverage was then normalized using the median value of all amplicons in that sample. Low quality samples and samples with a high coverage variability were removed. Then, systematic differences among amplicons were normalized. Copy number gains and losses were identified using 99% confidence intervals calculated per gene. The algorithm does not require normal samples to be included; but to obtain reliable results, multiple tumor samples should be included for a more robust and accurate normalization, and to make a better estimation of the 99% confidence intervals per gene. In addition, the algorithm assumes that each amplicon or gene is gained or deleted in a minority of the samples. Copy number analysis, visualization of results, loss of heterozygosity, and chromosomal imbalances were done using the Next-Generation Sequencing Expert shiny app (<https://git.lumc.nl/druano/NGSE>)

The detection of copy number variation by DNA NGS was validated by comparing the data from in situ hybridization and IHC (Fig. 2). Sample-to-data time was 5 days to 7 days.

RNA Next-Generation Sequencing

RNA NGS was performed with the Archer Comprehensive Thyroid and Lung panel. This method is capable of detecting fusions with a novel or unknown fusion partner using gene-specific primers in conjunction with molecular barcoded adapters. The RNA NGS panel produces NGS libraries targeting *ALK*, *AXL*, *BRAF*, *CCND1*, *EGFR*, *FGFR1*, *FGFR2*, *FGFR3*, *MET*, *NTRK1*, *NTRK2*, *NTRK3*, *NRG1*, *PPARG*, *RAF1*, *RET*, *ROS1*, and *THADA*, including detection of *MET* exon 14 skipping events. In addition, the RNA NGS panel can detect mutations in *ALK*, *AKT1*, *BRAF*, *CTNNB1*, *DDR2*, *EGFR*, *ERBB2*, *FGFR1*, *GNAS*, *HRAS*, *IDH1*, *IDH2*, *KRAS*, *MAP2K1*, *NRAS*, *NTRK1*, *PIK3CA*, *RET*, and *ROS1*. Moreover, imbalances in *ALK*, *NTRK1*, *NTRK2*, *NTRK3*, *RET*, and *ROS1* can be identified. RNA NGS required 20 ng to 200 ng nucleic acid per reaction. Both fresh frozen and FFPE tissue were used. The generated libraries were sequenced using an Ion Torrent platform and the produced reads were analyzed using the Comprehensive Thyroid and Lung Target Region File and the vendor supplied software (Archer Analysis, version 5.1.7). The sample-to-data time was 5 days.

Statistical Analysis

Statistical analysis was performed using IBM SPSS Statistics software, version 25. We defined pathogenic driver mutations as class 4 or 5 pathogenic mutations in *KRAS*, *EGFR*, *BRAF*, *ERBB2*; high amplifications in *ERBB2* and *EGFR*; fusions in *ALK*, *ROS1*, *RET*, *NTRK1*, 2, and 3, and *FGFR1*, 2, and 3; *MET* exon 14 skipping and *BRAF*

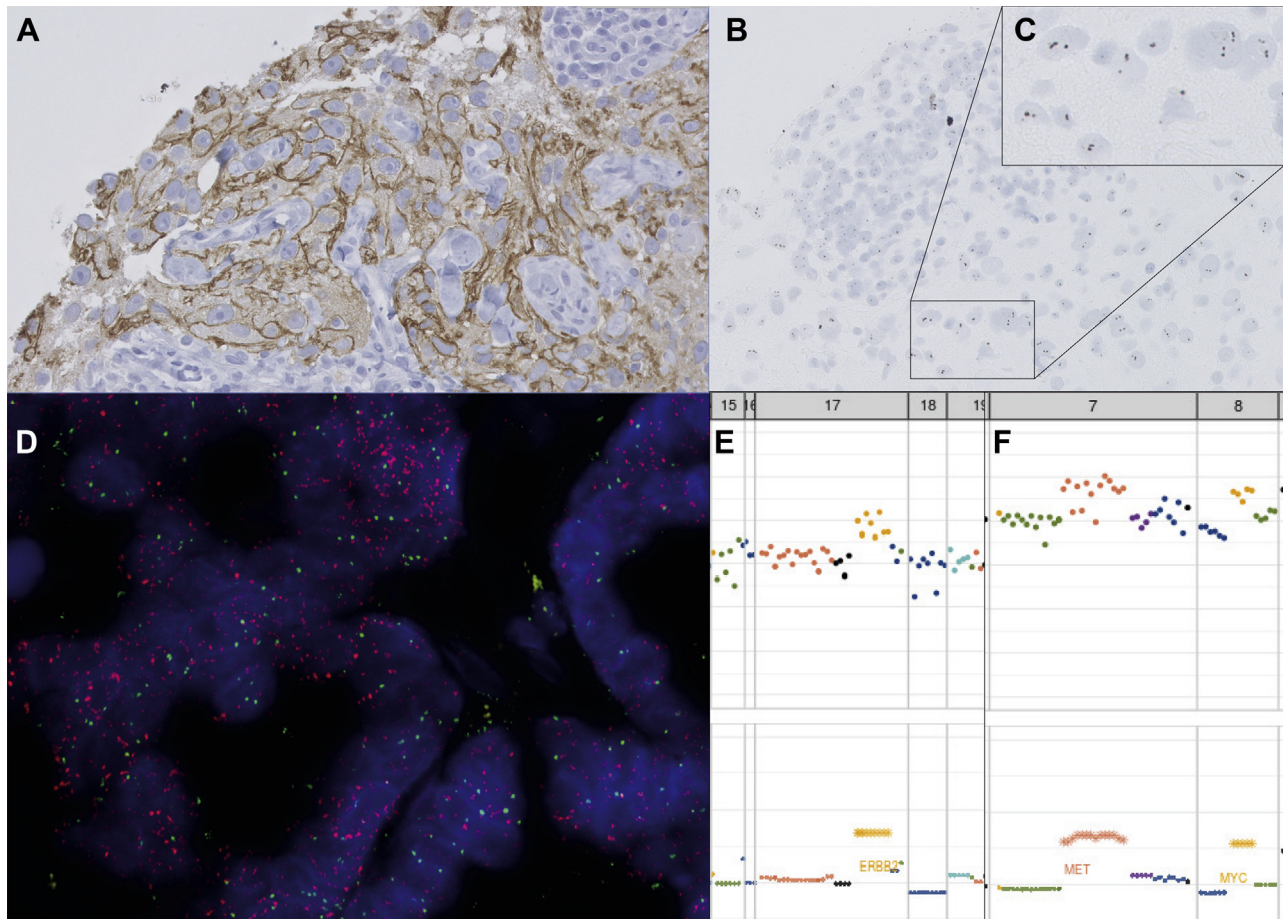


Figure 2. Copy number variation analysis for *ERBB2* and *MET* amplification. (A) *ERBB2* staining using immunohistochemistry; (B) *ERBB2* silver-stained in situ hybridization; (C) enlargement of (B). (D) *MET* fluorescence in situ hybridization: green, centromere SE7 probe on chromosome 7; red, *MET* probe showing high *MET* amplification with >10 signals per cluster per cell; (E) DNA next-generation sequencing read count of chromosome 13 to 21, with *ERBB2* amplification on chromosome 17 (upper panel: logarithmic scale, each dot representing the median read count per amplicon, lower panel: normalized read counts); (F) DNA next-generation sequencing read count of chromosome five to eight, with *MET* amplification on chromosome 7 and *MYC* amplification on chromosome 8 (upper panel: logarithmic scale, each dot representing the median read count per amplicon, lower panel: normalized read counts).

exon skipping. Class 3 mutations of unknown pathogenicity were not taken into account.

Ethics

Informed consent was obtained from the patients in the two illustrated cases. The rest of the data were obtained from routine diagnostic reports and were anonymized before processing.

Results

Case Characteristics

Cases from March 2018 until January 2019 were included. From March 2018 until September 2018, 192 cases were enrolled in cohort 1 and were evaluated with the parallel approach (Fig. 1). From September 2018 until January 2019, 198 cases were enrolled in cohort 2 and were evaluated with the sequential

approach. Both groups had similar characteristics as outlined in Table 1.

DNA Next-Generation Sequencing

DNA NGS identified mutations in oncogenes in 241 of the 375 successfully screened cases (64.3%), as also outlined in Table 2, including: *KRAS* (33.3%), *EGFR* (11.2% mutation and 2.9% amplification), *ERBB2* (2.1% mutation and 1.1% amplification), *BRAF* (5.1%), *PIK3CA* (2.9%), *NRAS* (1.6%), *MAP2K1* (1.1%), *MET* (0.8% mutation, 1.1% amplification, and 0.3% exon 14 skipping).

Genomic aberrations were also found in tumor suppressor genes, for example, in *TP53* (48.8%), *STK11* (8.3%), *CDKN2A* (4.0% mutation and 5.6% homozygous deletion), *CTNNB1* (2.1%), *PTEN* (1.9%), and *RB1* (1.1% mutation and 0.5% deletion).

MET exon 14 skipping was detected by DNA NGS in only one case. The ability to detect *MET* exon 14 skipping

Table 1. Case Characteristics

Characteristic	Cohort 1: Parallel Approach (n = 192)	Cohort 2: Sequential Approach (n = 198)	p Value
Patient characteristics			
Age	67.3 (43-86)	67.5 (31-90)	0.83
Female	82 (43%)	99 (50%)	0.16
Male	110 (57%)	99 (50%)	0.16
Smoking status			
Never smoker	22 (11%)	24 (12%)	0.49
Former smoker	73 (38%)	89 (45%)	
Current smoker	80 (42%)	71 (36%)	
Unknown	17 (9%)	14 (7%)	
Tumor type			
Adenocarcinoma	174 (91%)	182 (92%)	0.46
NSCLC NOS	14 (7%)	11 (6%)	
Adenosquamous	4 (2%)	3 (2%)	
Pleiomorphic	0	2 (1%)	
Tissue origin			
Primary tumor	63 (33%)	70 (35%)	0.61
Lymph node	59 (31%)	68 (34%)	
Pleural fluid	22 (11%)	17 (9%)	
Distant metastasis	48 (25%)	43 (22%)	
Sample type			
Cytology	76 (40%)	74 (37%)	0.68
Histology	116 (60%)	124 (63%)	
PD-L1 status			
Negative (<1%)	88 (46%)	83 (42%)	0.37
Low positivity (1%-49%)	33 (17%)	43 (22%)	
High positivity (50%-100%)	47 (25%)	52 (26%)	
Insufficient tissue available	6 (3%)	9 (5%)	
Unknown (performed elsewhere)	18 (9%)	11 (6%)	

In cohort 1, both DNA NGS and RNA NGS were performed on all specimens. In cohort 2, DNA NGS was performed on all specimens, and when no pathogenic driver mutation in KRAS, BRAF, EGFR, or ERBB2; MET exon 14 skipping; or amplification in EGFR and ERBB2 was found, RNA NGS was performed. The *p* value for age was calculated with an unpaired *t* test, all other *p* values were calculated with Pearson chi-square test. NOS, not otherwise specified; NGS, next-generation sequencing; PD-L1, programmed death-ligand 1.

Table 2. Different Characteristics and Outcomes for Never Smokers Compared with Former and Current Smokers

Characteristic	Never Smokers (n = 46)	Former and Current Smokers (n = 313)	p Value
Patient characteristics			
Female	26 (61%)	138 (44%)	0.04
Male	18 (39%)	175 (56%)	0.04
Age	67.9 (31-89)	67.5 (43-90)	0.81
DNA NGS			
Driver identified	26 (59%)	175 (58%)	0.01
Tumor suppressor or copy number variance only	7 (16%)	95 (32%)	
No mutations	11 (35%)	32 (11%)	
RNA NGS			
Fusion and exon skipping	10 (32%)	7 (4%)	0.00
No fusions	21 (68%)	182 (96%)	

DNA NGS was performed successfully in never smokers in 44 cases and in former and current smokers in 302 cases. RNA NGS was performed successfully in never smokers in 31 cases and in former and current smokers in 270 cases. NGS, next-generation sequencing.

in DNA NGS depends on the location of the splice-inducing mutation at the splice acceptor site in intron 13 or the splice donor site at intron 14. DNA NGS using the applied cancer hotspot panel does not cover the complete splice region involved in *MET* exon 14 skipping, explaining the four additional cases of *MET* exon 14 skipping identified with RNA NGS.

When comparing our data with The Cancer Genome Atlas (TCGA)⁵³ and Memorial Sloan Kettering-Integrated Mutation Profiling of Actionable Targets (MSK-IMPACT)³⁶ datasets, we found that our data were mostly concordant with data from these databases. The observed differences were most likely because of the inclusion in TCGA of a more limited range of TNM stages and, therefore, include fewer tumor progression-related mutations. TCGA and MSK-IMPACT included tumors from patients with more diverse international origins, whereas we received cases from hospitals in only the western part of the Netherlands. In addition, we excluded *EGFR* tyrosine kinase inhibitor (TKI)-resistant cases, but the MSK-IMPACT database included tumors

harboring *EGFR* T790M mutations, resulting in MSK-IMPACT having a higher percentage of *EGFR* mutations than our dataset. In Figure 3, we provide a chart showing the most frequently seen and the most therapeutic relevant pathogenic mutations.

RNA Next-Generation Sequencing

In the sequential approach, additional RNA NGS was necessary in 105 of 198 cases without a mutagenic driver (53%), whereas it was performed in all 192 cases in the parallel approach.

In both cohorts combined, RNA NGS was performed in 297 cases. Fusions were found in 19 cases, representing 6.4% of all RNA NGS cases and 4.9% of the total cohort. *ALK* fusions were detected in eight cases, of which *EML4* was the most common fusion partner ($n = 6$). In one case, *ALK* was fused to *STRN3*, and in another case to *RPTOR*. In all *EML4* and *STRN3* fusion cases, the *ALK* breakpoint was at exon 20. In the *RPTOR* fusion case, the breakpoint was at *ALK* exon 10 and the fusion protein was out of frame, which also explains the *ALK*-negative IHC. Because there was no other pathogenic mutation, this fusion was reported, but it is not certain if this is an oncogenic driver. Therefore, the patient has not been treated with TKIs and response data are not available. *KIF5B-RET* fusion occurred in two cases, *FGFR3* fusion occurred in two cases (with *TACC3* and

WHSC1), *MET* exon 14 skipping occurred in four additional cases (one case already identified with DNA NGS), and *CD74-ROS1* fusion occurred in one case (Fig. 4).

Fusion-positive cases were mutually exclusive with pathogenic driver mutations in both cohorts, as shown in Figure 4. We did, however, find co-occurrence of *ALK* fusions with *CDKN2A* and *NOTCH1* deletions and *MDM2* and *CDK4* amplifications. *MET* exon 14 skipping co-occurred with *CDKN2A* deletions, and *TP53*, *APC*, and *PTEN* mutations, *RET* fusion with *TP53* mutations, and *FGFR3* fusion coincided with *TP53* and *STK11* mutations. *BRAF* exon skipping coincided with non-V600 *BRAF* mutations and *STK11* mutations. However, the non-V600 *BRAF* mutation was a very low frequency variant and was only observed in RNA NGS.

Never-Smoking Status

In this study, 22 never smokers were included in the parallel cohort and 24 in the sequential cohort. These patients had significantly different characteristics (more often female, $p = 0.04$) and demonstrated a different outcome from DNA NGS and RNA NGS, compared with former and current smokers ($n = 313$), as outlined in Table 2. Smoking history was unknown in 31 cases, which were not included in Table 2.

Although a driver mutation was identified by DNA NGS equally often in never smokers, the types of driver mutations compared with former and current smokers were more often *EGFR* (41% in never smokers versus 7% in former- and current smokers, $p = 0.00$) and less often *KRAS* (9% in never smokers versus 37% in former- and current smokers, $p = 0.00$). Furthermore, a fusion was found more often in never smokers (32%) versus former and current smokers (4%) ($p = 0.00$) (Fig. 5).

In never smokers, DNA NGS failed and a new biopsy was recommended in two cases. In the cases in which DNA NGS was successful, an oncogenic driver was identified in 26 cases (59%). In the 18 cases (41%) in which no oncogenic driver was found in DNA NGS, an oncogenic fusion was found in 10 of 13 successfully analyzed cases (77%). RNA NGS failed in five cases, and a new biopsy was recommended.

In some of the patients included in the never-smoking group, we registered smoking-associated mutations, for example four *KRAS* mutations. One patient with *KRAS* mutation had never smoked, but it was mentioned in the file that this patient had had frequent exposure to second-hand smoke. This might also have been the case in other patients with *KRAS* mutations; but this was not always registered extensively in their case file.

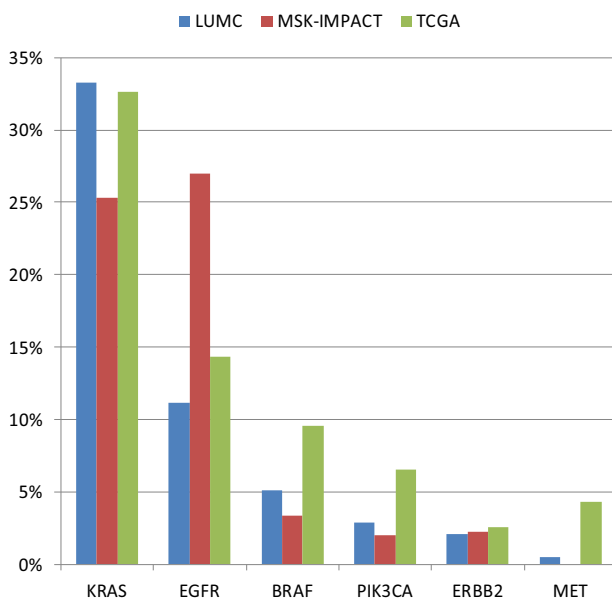


Figure 3. Comparison of mutation prevalence in the dataset from The Cancer Genome Atlas-NSCLC adenocarcinoma, Memorial Sloan Kettering-Integrated Mutation Profiling of Actionable Targets, and Leiden University Medical Centre (both cohorts combined). Y axis: percentage of all cases, x axis: oncogenic somatic mutation.

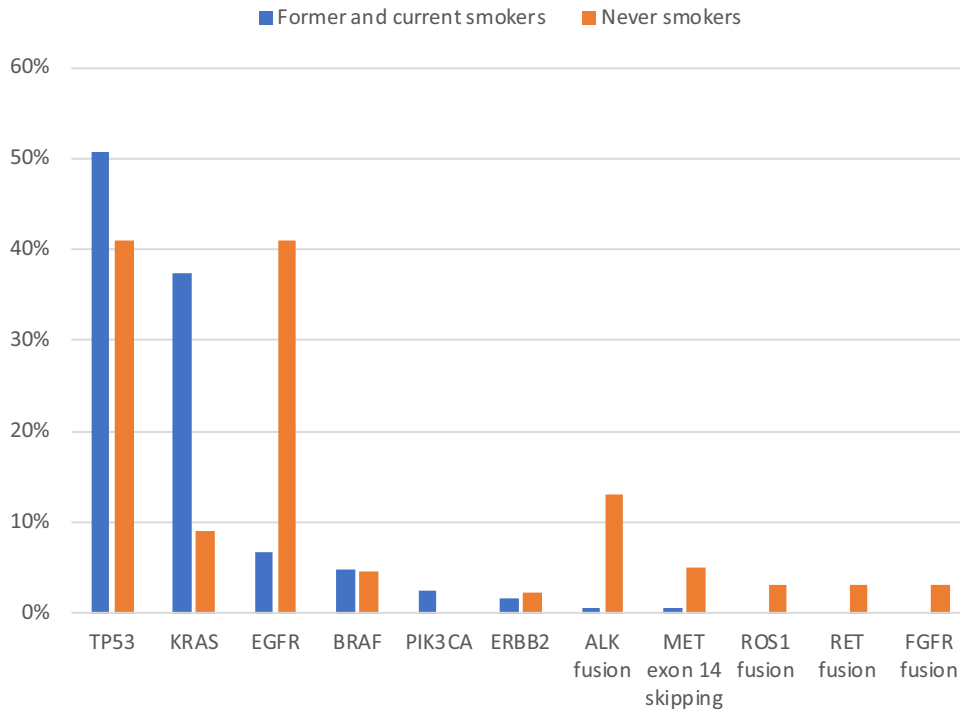


Figure 5. Mutations found in smokers (blue) versus never smokers (orange). The difference is significant for *KRAS* ($p = 0.00$), *EGFR* ($p = 0.00$), and *ALK* ($p = 0.00$). Only successful next-generation sequencing (NGS) analyses were taken into account. For smokers $n = 375$ for DNA NGS targets and $n = 270$ for RNA NGS targets; for never smokers $n = 44$ for DNA NGS targets and $n = 31$ for RNA NGS targets.

before the DNA NGS or RNA NGS results were confirmed to start crizotinib therapy without delay.

In one case, insufficient material was available for IHC, but an *ALK* fusion was found in RNA NGS performed on cytology slides. In another case, *ALK* was negative in IHC, and a *RPTOR-ALK* fusion was found in RNA NGS. However, in this fusion, the *ALK* breakpoint was in exon 10 instead of in exon 20 or 19, as is usually seen. This fusion resulted in an inactive protein and therefore did not lead to *ALK* overexpression that can be detected by *ALK* IHC.

NGS Challenges and the Failure to Complete Molecular Workups

The overall dropout rate of DNA NGS was lower (4%, $n = 13$) than the overall dropout rate of RNA NGS (18%, $n = 54$). Of these cases, a driver alteration had already been identified by DNA NGS in 18 cases (33%). Of the remaining cases in which no DNA NGS data with driver mutation and no RNA NGS data could be generated ($n = 44$ [67%, or 11% of the total cohort]), nine cases were eligible for immunotherapy on the basis of PD-L1 expression. An additional biopsy was recommended

Table 3. Turnaround Time for Each Cohort

Cohort	Characteristic	MD Time	MD-to-Sign Time	Received-to Sign Time
Overall ($n = 390$)	Mean (range)	1906 (2-364)	21.1 (2-365)	33.6 (7-2285)
	Median	9	10	13
Parallel cohort ($n = 192$)	Mean (range)	14.3 (5-364)	15.7 (6-365)	19.7 (7-365)
	Median	9	10	13
Sequential cohort ($n = 198$)	Mean (range)	24.7 (2-182)	26.3 (2-186)	47 (7-2285)
	Median	9	10	14
Sequential cohort without RNA NGS ($n = 90$)	Mean (range)	7.2 (2-20)	9.1 (2-59)	16.1 (7-277)
	Median	7	8	9
Sequential cohort with RNA NGS ($n = 108$)	Mean (range)	39.3 (6-182)	40.6 (6-186)	72.8 (7-2285)
	Median	15	15	21

MD time: number of workdays from the request for DNA NGS or RNA NGS by the pathologist until all data from molecular diagnostics were available. MD-to-sign time: number of workdays from the request for DNA NGS or RNA NGS by the pathologist until the final report is sent to the clinician. Received-to-sign time: number of workdays from the arrival of the tissue at the pathology department until the final report is sent to the clinician. Outliers in the third category are mostly owing to late metastasis cases. Outliers in the first and second column are mostly because of late additional RNA NGS in the startup phase of this study. NGS, next-generation sequencing; MD, molecular diagnostics.

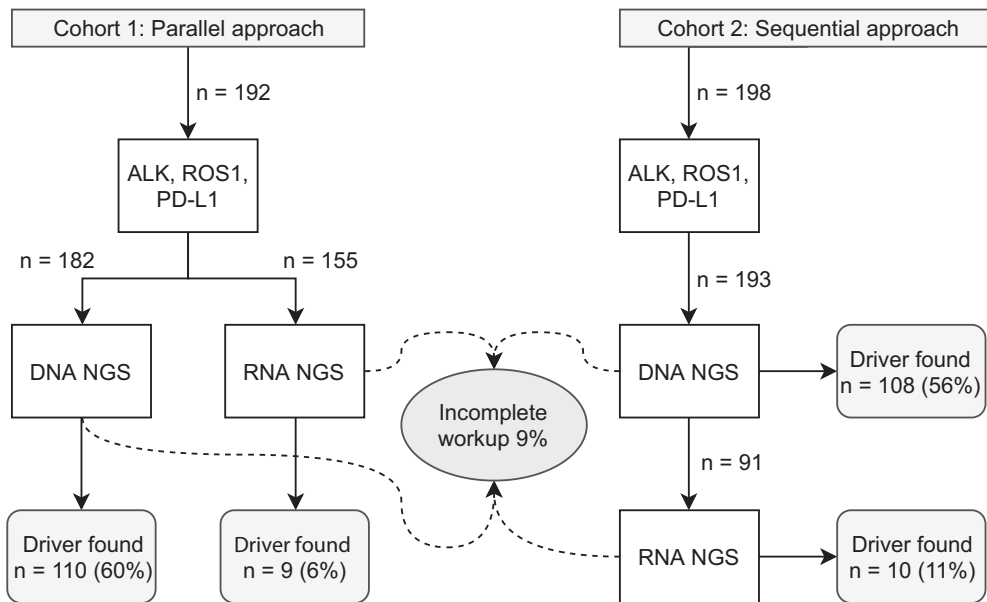


Figure 6. Drivers found in the sequential and parallel approaches. The workup was incomplete in 9% of all cases, and a new biopsy was recommended.

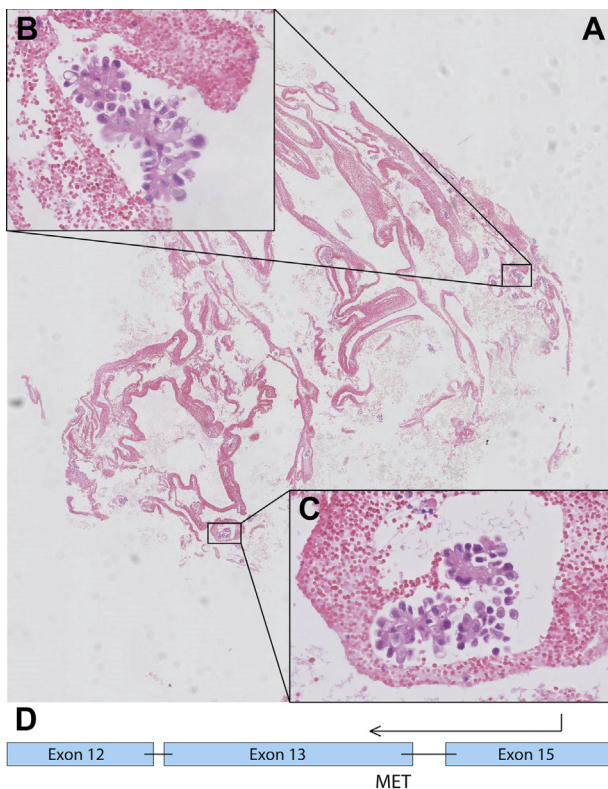


Figure 7. Case 1, a 70-year-old man presenting with stage IV NSCLC with positive pleural and pericardial effusions. (A) Hematoxylin and eosin staining of hemorrhagic pericardial fluid with tumor islets that was used for DNA next-generation sequencing (NGS) and RNA NGS; (B, C) enlarged sections of (A); (D) RNA NGS readout showing the *MET* exon 14 splicing event.

owing to RNA NGS failure in 35 cases (9% of the total cohort) (Fig. 6).

Cytology

Among all cytology samples (n = 150), DNA NGS did not generate reliable data in nine samples (6%) . RNA NGS could not be executed in 45 samples (30%), mainly because of the limited number of tumor cells that were available in the specimen. RNA NGS requires 20 ng to 200 ng of nucleic acid, whereas DNA NGS only requires 15 ng.

Decalcification

RNA NGS failed in 10 cases (45%) of the decalcified tissues, and six cases (27%) were likewise not suitable for DNA NGS. This was most likely caused by the destruction of nucleic acid by conditions encountered during the decalcification procedure. Fusions detected in small cytology samples were illustrated by the following cases:

Case 1. A 70-year-old man presented at the emergency room with cardiac tamponade and pleural effusion. Pericardiocentesis was performed and the drained fluid was analyzed by a pathologist. A thyroid transcription factor-1-positive adenocarcinoma was discovered in the pericardial fluid and in the pleural fluid. The adenocarcinoma proved to be *ALK*- and *ROS1*-negative; the PD-L1 tumor proportion score was 70%. DNA NGS revealed two pathogenic mutations in *TP53* and *CDKN2A*.

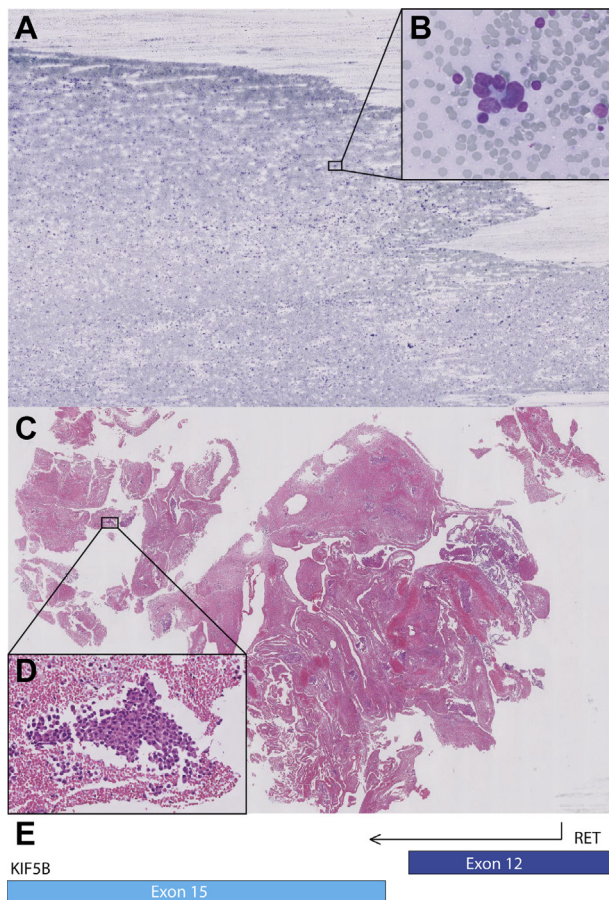


Figure 8. Case 2, a 60-year-old man who had never smoked, presenting with multiple nodal, osseous, ocular and subcutaneous metastases of a thyroid transcription factor-1-positive NSCLC. (A) Giemsa staining of a lymph node puncture that was used for the molecular workup, including DNA next-generation sequencing (NGS) and RNA NGS; (B) enlargement of (A); (C) cellblock with hematoxylin and eosin staining of a lymph node puncture that was used for immunohistochemistry; (D) enlargement of (C); (E) RNA NGS readout revealing a *KIF5B-RET* fusion.

Subsequent RNA NGS analysis revealed the presence of a *MET* exon 14 skipping event. The patient was treated with pembrolizumab, initially establishing a progression-free period; but after a few months the disease progressed, and the patient was included in the Drug Rediscovery Protocol trial (NCT02925234) to receive targeted *MET* exon 14 therapy. Full molecular workup was successfully performed on cytology samples with relatively low tumor cell percentage in this case (Fig. 7).

Case 2. A 60-year-old man presented with loss of vision in his right eye. An ocular tumor of unknown origin was discovered. In the workup, a thoracic computed tomography was performed. Multiple masses in both lungs, the mediastinum, the kidneys, and subcutis were

seen. The patient had never smoked and had no symptoms except mild intermittent back pain. An endobronchial ultrasound-guided lymph node puncture was conducted, and an examination by the pathologist revealed a thyroid transcription factor-1-positive adenocarcinoma. *ALK* and *ROS1* were negative, and PD-L1 was positive in 5% to 10% of the tumor cells. DNA NGS revealed no class 4 or class 5 pathogenic mutations. Fusion analysis by RNA NGS revealed a *KIF5B-RET* fusion, with the *RET* breakpoint at exon 12 and the *KIF5B* breakpoint at exon 15. Initial chemotherapeutic and immunotherapeutic regimens did not lead to stable disease or therapeutic response, and the patient was included in the Dutch Drug Rediscovery Protocol trial (NCT02925234) for *RET*-targeted treatment. Full molecular workup was successfully performed on a mediastinal lymph node fine-needle aspiration (FNA) sample (Fig. 8).

Discussion

Successful testing for the complex array of molecular targets in metastatic NSCLC demands careful molecular workup and judicious use of diagnostic IHC. For many laboratories, finding a way to navigate the many diagnostic options while not exhausting the tumor tissue of small biopsies or cytology samples remains a challenging task. To be “lean and mean” in molecular diagnostics and to become future-proof, laboratories will have to reduce their number of diagnostic steps in this extensive workup.

In this study, we present our in-house molecular workup for NSCLC that uses both DNA NGS and RNA NGS combined with IHC. To optimize our procedure, we compared a cohort in which we performed parallel DNA NGS and RNA NGS to a cohort in which DNA NGS was followed by RNA NGS only when no driver mutations were detected by DNA NGS in *KRAS*, *BRAF*, *EGFR*, or *ERBB2* (including *EGFR* and *ERBB2* amplification), or *MET* exon 14 skipping. Our results revealed that RNA NGS is a valuable addition to detect fusions for all relevant target sites (*ALK*, *ROS*, *RET*, *MET* exon 14 skipping, *BRAF* exon skipping, *NTRK*, and *FGFR*), especially in never smokers. We also observed that RNA NGS is able to identify known fusion partners (e.g., *EML4-ALK* or *KIF5B-RET*) and novel or unusual partners (e.g., *RPTOR-ALK* and *TACC3-FGFR3*).

Additional RNA NGS changed treatment options in 5% of all cases and in 22% for never smokers. These data were in line with the recent study of Benayed et al.⁴⁹ who reported that even in large panels such as MSK-IMPACT, additional RNA NGS is required to identify all fusions and exon-skipping events, especially in cases without a clear driver and with a low tumor mutational

burden. Their study reported that in 39.4% of all cases in which the MSK-IMPACT could not identify a driver mutation, sufficient quality and quantity material was left for RNA NGS.

In concordance with the TCGA data, all detected fusions were mutually exclusive with pathogenic driver mutations in *EGFR*, *BRAF*, *KRAS*, *MET*, and *ERBB2*, supporting the sequential approach, as presented in Figure 1.⁵³ This sequential approach reduced the number of RNA NGS analyses by 47.0%.

The sequential approach had a median sample-to-data time of 9 days, which was the same as the parallel approach. However, in cases in which additional RNA NGS was required, the median turnaround time in the sequential approach was 15 days, versus 7 working days in cases in which this was not required. In our laboratory, the alternative of without RNA NGS—that is, DNA NGS with additional FISH and PCR analysis—would take approximately 8 days to 12 days.

When we take into account the cost of the parallel versus the sequential approach, the parallel approach is approximately twice as expensive. DNA NGS costs are estimated at €607, and RNA NGS costs at €500 to €700. Omitting RNA NGS in patients with a clear oncogenic driver in DNA NGS is possible in 47% of all cases, which considerably reduces the average costs of the molecular workup in NSCLC. However, the longer turnaround time is an important disadvantage of the sequential approach.

Moreover, in former and current smokers, the yield of additional RNA NGS is quite low: only seven fusions were found in 313 patients (2%); and because of the IHC screening for *ALK*, the turnaround time can be reduced in *ALK*-positive cases. This combination of low RNA NGS yield, high costs, and limited extension of the turnaround time justifies a sequential approach in former and current smokers.

In never smokers, 10 of 46 patients (22%) of all patients harbor a fusion, which can only be detected by RNA NGS. In addition, smokers only represent 12% of all patients presenting with advanced metastatic NSCLC. The higher yield of RNA NGS in this small group of patients asks for a parallel approach, and greater cost is not a sufficient argument to defer to a sequential approach in these patients. We, therefore, suggest a separate, parallel approach for never smokers, which is outlined in Figure 9.

More importantly, the combined DNA NGS and RNA NGS workup presented in this study is feasible on small tissue samples and cytology specimens. This is essential for daily clinical practice because in most laboratories, approximately 30% of NSCLC is diagnosed with cytology FNA samples. Our data found that the overall dropout rate was 4% in DNA NGS and 18% in RNA NGS. Cytology samples revealed slightly higher failure rates, with 6% in DNA NGS and 30% in RNA NGS, owing to the higher nucleic acid input required in RNA NGS (20 ng–200 ng) versus DNA NGS (only 15 ng). Overall, in 9% of cases, no driver mutation was found in DNA NGS and insufficient material was left for RNA NGS. In these cases, an additional biopsy was advised.

When comparing our method to large hybrid capture platforms, such as Foundation One, MSK-IMPACT, and MSK-Fusion, our dropout rate is low, especially when taking into account the fact that we made extensive use of cytology samples.^{49,50} The advantages of large panels such as Foundation One can only be harvested for cases with extensive amounts of tissue available. With Foundation One, only 60.9% of all samples of histologic confirmed NSCLC passed the preanalytical quality control check and were evaluable by the NGS assay.⁴⁹

It is important to mention that this workup performs optimally and is most tissue sparing when working with total nucleic acid (isolated in one procedure), so that

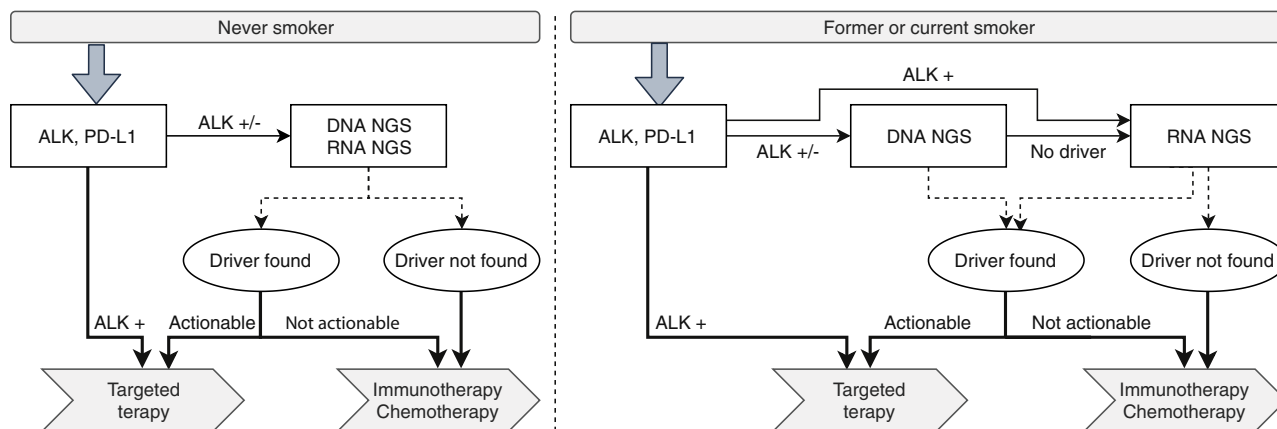


Figure 9. Proposed diagnostic process coming from data presented in this article. Left: never smokers; Right: former or current smokers.

tissues have to be cut only once. We isolated total nucleic acid in a single procedure using the tissue preparation system Siemens robot. Separate isolation of DNA and RNA would require more tumor material, possibly resulting in a higher dropout percentage.

As saving tissue is very important in the workup of advanced NSCLC, we should consider omitting *ROS1* IHC. This is mainly owing to the fact that the false-positive rate of *ROS1* IHC is so high that therapy can never be started without confirmation by RNA NGS. Thus, the only benefit would be that when *ROS1* IHC is positive, RNA NGS is started without delay and the *ROS1* cases are diagnosed more rapidly. However, the disadvantages are considerable, as the number needed to screen is very high, and in all these cases, valuable tissue is wasted.

A possible disadvantage of our method could be the lower sensitivity of DNA NGS for the detection of copy number variance. Detection of amplifications can be problematic especially in specimens with low tumor cell percentages. This was probably illustrated in the lower number of amplifications compared with TCGA and MSK-IMPACT data, as outlined in Figure 3. In some selected cases, for example, in the workup of post-*EGFR*-TKI resistance (which was not included in this study), additional *ERBB2* or *MET* FISH might be necessary if no resistance mutations (*T790M* and *C797S*) or other resistance mechanisms are detected.

We foresee an increasing need for RNA NGS in the postosimertinib resistance setting, as a wide variety of resistance mechanisms have been described, including fusions.⁴⁵ The ability to work with small sample sizes in this clinical setting is even more important, as the diagnostic workup for *EGFR*-TKI resistance mechanisms is often based on small core needle biopsies or FNA samples of growing metastatic sites. Our method, in which DNA NGS and RNA NGS are combined, could be an ideal and a practical choice for many laboratories dealing with this growing patient category.

In the future, we might further narrow the number of cases in which additional RNA NGS will be required, because tumors harboring pathogenic mutations in oncogenic driver genes such as *PIK3CA*, *HRAS*, *MAP2K1*, *MAP2K4*, *FGFR1*, *GNAS*, or *NRAS*, do not co-occur with fusion genes or *MET* exon 14 skipping, as reported in this cohort and the recent article by Benayed et al.⁴⁹ However, because both fusions and these somatic driver mutations are quite rare, more experience with molecular diagnostics in NSCLC is needed before we can be certain about the mutual exclusiveness of these rare driver mutations.

In conclusion, we have described our optimization procedure for the molecular workup of advanced-stage NSCLC through a sequential approach for former and current smokers using IHC and DNA NGS followed by

RNA NGS in a selected subset of cases without detectable activating mutations in *KRAS*, *BRAF*, *EGFR*, *ERBB2*, or *MET* exon 14 skipping.

Switching to a sequential approach drastically reduced the number of unnecessary diagnostic steps and the accompanying costs, as additional RNA NGS was necessary in only 53% of all cases. In never smokers (12% of all patients), we support a parallel approach, because RNA NGS has a much higher yield. More importantly, our method is feasible and successful for small samples, including that of cytologic material, making it an ideal solution for laboratories that want to step away from the classical workup for NSCLC, which combines NGS with multiple FISH analyses, but that do not work with the large sample sizes necessary for large (and more expensive) hybrid capture panels or whole-genome sequencing. In summary, the method presented in this article may drastically reduce the complexity and number of diagnostic steps and can also provide flexibility in the constantly evolving landscape of actionable targets in NSCLC.

Acknowledgments

The authors thank Karin Kleiverda, Katherine Vahl-Harding, Juanita Ippel and Kim van Elst for their substantial help in collecting data for this study. ArcherDX Inc. supplied 24 reactions free of charge to finish this study.

Supplementary Data

Note: To access the supplementary material accompanying this article, visit the online version of the *Journal of Thoracic Oncology* at www.jto.org and at <https://doi.org/10.1016/j.jtho.2020.01.019>.

References

1. Bray F, Ferlay J, Soerjomataram I, Siegel RL, Torre LA, Jemal A. Global cancer statistics 2018: GLOBOCAN estimates of incidence and mortality worldwide for 36 cancers in 185 countries. *CA Cancer J Clin*. 2018;68:394-424.
2. Howlader N, Noone AM, Krapcho M, et al. Contents of the SEER Cancer Statistics Review (CSR), 1975-2016. Bethesda, MD, National Cancer Institute; 2019. Bethesda, MD, US Department of Health and Human Services.
3. Paez JG, Jänne PA, Lee JC, et al. *EGFR* mutations in lung cancer: correlation with clinical response to gefitinib therapy. *Science*. 2004;304:1497-1500.
4. Lynch TJ, Bell DW, Sordella R, et al. Activating mutations in the epidermal growth factor receptor underlying responsiveness of non-small-cell lung cancer to gefitinib. *N Engl J Med*. 2004;350:2129-2139.
5. Cardarella S, Ogino A, Nishino M, et al. Clinical, pathologic, and biologic features associated with *BRAF* mutations in non-small cell lung cancer. *Clin Cancer Res*. 2013;19:4532-4540.

6. Planchard D, Kim TM, Mazieres J, et al. Dabrafenib in patients with BRAF(V600E)-positive advanced non-small-cell lung cancer: a single-arm, multicentre, open-label, phase 2 trial. *Lancet*. 2016;17:642-650.
7. Hyman DM, Puzanov I, Subbiah V, et al. Vemurafenib in multiple nonmelanoma cancers with BRAF V600 mutations. *N Engl J Med*. 2015;373:726-736.
8. Stephens P, Hunter C, Bignell G, et al. Lung cancer: intragenic ERBB2 kinase mutations in tumours. *Nature*. 2004;431:525-526.
9. Mazières J, Peters S, Lepage B, et al. Lung cancer that harbors an HER2 mutation: epidemiologic characteristics and therapeutic perspectives. *J Clin Oncol*. 2013;31:1997-2003.
10. Skoulidis F, Byers LA, Diao L, et al. Co-occurring genomic alterations define major subsets of KRAS-mutant lung adenocarcinoma with distinct biology, immune profiles, and therapeutic vulnerabilities. *Cancer Discov*. 2015;5:860-877.
11. Skoulidis F, Goldberg ME, Greenawalt DM, et al. STK11/LKB1 mutations and PD-1 inhibitor resistance in KRAS-mutant lung adenocarcinoma. *Cancer Discov*. 2018;8:822-835.
12. Awad MM, Oxnard GR, Jackman DM, et al. MET exon 14 mutations in non-small-cell lung cancer are associated with advanced age and stage-dependent MET genomic amplification and c-MET overexpression. *J Clin Oncol*. 2016;34:721-730.
13. Frampton GM, Ali SM, Rosenzweig M, et al. Activation of MET via diverse Exon 14 splicing alterations occurs in multiple tumor types and confers clinical sensitivity to MET inhibitors. *Cancer Discov*. 2015;5:850-859.
14. Heist RS, Shim HS, Gingipally S, et al. MET Exon 14 skipping in non-small cell lung cancer. *Oncologist*. 2016;21:481-486.
15. Paik PK, Drilon A, Fan PD, et al. Response to MET inhibitors in patients with stage IV lung adenocarcinomas harboring MET mutations causing exon 14 skipping. *Cancer Discov*. 2015;5:842-849.
16. Hirsch FR, Varella-Garcia M, McCoy J, et al. Increased epidermal growth factor receptor gene copy number detected by fluorescence in situ hybridization associates with increased sensitivity to gefitinib in patients with bronchioloalveolar carcinoma subtypes: a Southwest Oncology Group Study. *J Clin Oncol*. 2005;23:6838-6845.
17. Hirsch FR, Varella-Garcia M, Bunn PA Jr, et al. Epidermal growth factor receptor in non-small-cell lung carcinomas: correlation between gene copy number and protein expression and impact on prognosis. *J Clin Oncol*. 2003;21:3798-3807.
18. Gautschi O, Milla J, Filleron T, et al. Targeting RET in patients with RET-rearranged lung cancers: results from the global, multicenter RET registry. *J Clin Oncol*. 2017;35:1403-1410.
19. Kohno T, Ichikawa H, Totoki Y, et al. KIF5B-RET fusions in lung adenocarcinoma. *Nat Med*. 2012;18:375-377.
20. Sabari JK, Offin MD, Wu SL, et al. RET-rearranged lung cancers: immunophenotype and response to immunotherapy. *J Clin Oncol*. 2018;36:9034-9034.
21. Kwak EL, Bang YJ, Camidge DR, et al. Anaplastic lymphoma kinase inhibition in non-small-cell lung cancer. *N Engl J Med*. 2010;363:1693-1703.
22. Shaw AT, Kim DW, Nakagawa K, et al. Crizotinib versus chemotherapy in advanced ALK-positive lung cancer. *N Engl J Med*. 2013;368:2385-2394.
23. Soda M, Choi YL, Enomoto M, et al. Identification of the transforming EML4-ALK fusion gene in non-small-cell lung cancer. *Nature*. 2007;448:561-566.
24. Hyman DM, Laetsch TW, Kummar S, et al. The efficacy of larotrectinib (LOXO-101), a selective tropomyosin receptor kinase (TRK) inhibitor, in adult and pediatric TRK fusion cancers. *J Clin Oncol*. 2017;35(suppl 18):LBA2501.
25. Farago AF, Taylor MS, Doebele RC, et al. Clinicopathologic features of non-small-cell lung cancer harboring an NTRK gene fusion [e-pub ahead of print]. *JCO Precis Oncol*. <https://doi.org/10.1200/PO.18.00037>, accessed July 23, 2018.
26. Bergethon K, Shaw AT, Ou SH, et al. ROS1 rearrangements define a unique molecular class of lung cancers. *J Clin Oncol*. 2012;30:863-870.
27. Shaw AT, Ou SH, Bang YJ, et al. Crizotinib in ROS1-rearranged non-small-cell lung cancer. *N Engl J Med*. 2014;371:1963-1971.
28. Garon EB, Rizvi NA, Rui R, et al. Pembrolizumab for the treatment of non-small-cell lung cancer. *N Engl J Med*. 2015;372:2018-2028.
29. Reck M, Rodríguez-Abreu D, Robinson AG, et al. Pembrolizumab versus chemotherapy for PD-L1-positive non-small-cell lung cancer. *N Engl J Med*. 2016;375:1823-1833.
30. Borghaei H, Paz-Ares L, Horn L, et al. Nivolumab versus docetaxel in advanced nonsquamous non-small-cell lung cancer. *N Engl J Med*. 2015;373:1627-1639.
31. Brahmer J, Reckamp KL, Baas P, et al. Nivolumab versus docetaxel in advanced squamous-cell non-small-cell lung cancer. *N Engl J Med*. 2015;373:123-135.
32. Smolle E, Pichler M. Non-smoking associated lung cancer: a distinct entity in terms of tumor biology, patient characteristics and impact of hereditary cancer predisposition. *Cancers (Basel)*. 2019;11:E204.
33. National Comprehensive Cancer Network. *NCCN Guidelines*. 3.2019 Version non-small cell lung cancer. https://www.nccn.org/professionals/physician_gls/default.aspx. Accessed March 1, 2019.
34. Herbst RS, Morgensztern D, Boshoff C. The biology and management of non-small cell lung cancer. *Nature*. 2018;553:446-454.
35. Sabari JK, Santini F, Bergagnini I, Lai WV, Arbour KC, Drilon A. Changing the therapeutic landscape in non-small cell lung cancers: the evolution of comprehensive molecular profiling improves access to therapy. *Curr Oncol Rep*. 2017;19:24.
36. Jordan EJ, Kim HR, Arcilla ME, et al. Prospective comprehensive molecular characterization of lung adenocarcinomas for efficient patient matching to approved and emerging therapies. *Cancer Discov*. 2017;7:596-609.
37. Barlesi F, Mazieres J, Merlio JP, et al. Routine molecular profiling of patients with advanced non-small-cell lung

- cancer: results of a 1-year nationwide programme of the French Cooperative Thoracic InterGroup (IFCT). *Lancet*. 2016;387:1415-1426.
38. Sholl LM. Molecular diagnostics of lung cancer in the clinic. *Transl Lung Cancer Res*. 2017;6:560-569.
 39. Sholl LM, Aisner DL, Varella-Garcia M, et al. Multi-institutional oncogenic driver mutation analysis in lung adenocarcinoma: the lung cancer mutation consortium experience. *J Thorac Oncol*. 2015;10:768-777.
 40. Lam SW, Cleton-Jansen AM, Cleven AHG, et al. Molecular analysis of gene fusions in bone and soft tissue tumors by Anchored Multiplex PCR-based targeted next-generation sequencing. *J Mol Diagn*. 2018;20:653-663.
 41. Zheng Z, Liebers M, Zhelyazkova B, et al. Anchored multiplex PCR for targeted next-generation sequencing. *Nat Med*. 2014;20:1479-1484.
 42. McLeer-Florin A, Duruisseaux M, Pinsolle J, et al. ALK fusion variants detection by targeted RNA-next generation sequencing and clinical responses to crizotinib in ALK-positive non-small cell lung cancer. *Lung Cancer*. 2018;116:15-24.
 43. Yoh K, Seto T, Satouchi M, et al. Vandetanib in patients with previously treated RET-rearranged advanced non-small-cell lung cancer (LURET): an open-label, multi-centre phase 2 trial. *Lancet Respir Med*. 2017;5:42-50.
 44. Driilon A, Fu S, Patel MR, et al. A phase I/IIb trial of the VEGFR-sparing multikinase RET inhibitor RXDX-105. *Cancer Discov*. 2018;9:384-395.
 45. Oxnard GR, Hu Y, Mileham KF, et al. Assessment of resistance mechanisms and clinical implications in patients with EGFR T790M-positive lung cancer and acquired resistance to osimertinib. *JAMA Oncol*. 2018;4:1527-1534.
 46. Vendrell JA, Taviaux S, Béganton B, et al. Detection of known and novel ALK fusion transcripts in lung cancer patients using next-generation sequencing approaches. *Sci Rep*. 2017;7:12510.
 47. Davies KD, Le AT, Sheren J, et al. Comparison of molecular testing modalities for detection of ROS1 rearrangements in a cohort of positive patient samples. *J Thorac Oncol*. 2018;13:1474-1482.
 48. Tafe LJ, de Abreu FB, Peterson JD, Tsongalis GJ, Exon M. 14 Skipping mutation in non-small cell lung cancer identified by anchored multiplex PCR and next-generation sequencing. *J Cancer Epidemiol Prev*. 2016;1:1.
 49. Benayed R, Offin M, Mullaney K, et al. High yield of RNA sequencing for targetable kinase fusions in lung adenocarcinomas with no driver alteration detected by DNA sequencing and low tumor mutational burden. *Clin Can Res*. 2019;25:4712-4722.
 50. Marino P, Touzani R, Perrier L, et al. Cost of cancer diagnosis using next-generation sequencing targeted gene panels in routine practice: a nationwide French study. *Eur J Hum Genet*. 2018;26:314-323.
 51. van Eijk R, Stevens L, Morreau H, van Wezel T. Assessment of a fully automated high-throughput DNA extraction method from formalin-fixed, paraffin-embedded tissue for KRAS, and BRAF somatic mutation analysis. *Exp Mol Pathol*. 2013;94:121-125.
 52. Thorvaldsdóttir H, Robinson JT, Mesirov JP. Integrative Genomics Viewer (IGV): high-performance genomics data visualization and exploration. *Brief Bioinform*. 2013;14:178-192.
 53. Cancer Genome Atlas Research Network. Comprehensive molecular profiling of lung adenocarcinoma. *Nature*. 2014;511:543-550.